Ice Cloud Particle Terminal Velocity Parameterizations for Temperatures of 0 to -85C

Andy Heymsfield

NCAR, Boulder, CO

At an ECMWF Workshop in 1994, Christian Jakob reported on the impact of ice particle sedimentation velocities on global climate radiative forcing and the Earth's net surface temperature. Fallspeeds of hydrometeors have a large effect on cloud lifetime and the Earth's radiation budget. In my presentation at the 2012 ECMWF Workshop, I reported on the microphysical properties of ice cloud layers formed directly or indirectly by deep convection and large-scale lifting were investigated using in situ observations from ten field programs. The end product of this study was to estimate the fallspeeds of ice particles as a function of size, altitude, and cloud formation mechanism: convective and stratiform. I'll focus this report on this end product because of its significance.

The data used in this study were collected at latitudes ranging from 12S to 70N (Fig. 1), longitudes from 148W to 130E, altitudes from near the surface to 18.7 km, and with temperatures from 0 to –86 C. The composite data set includes more than 85000 in-cloud size distributions, each spanning horizontal path lengths of 750–1000 m, or a total of about 800,000 km. Balloon-borne ascents through ice cloud layers are included in the data set. This data set is representative of the wide range of conditions where ice clouds are found in the troposphere and lower stratosphere on a near-global scale.

In general, particle habits for the convective situations exhibited light to moderate riming without graupel and the particles above about 500 microns were often aggregates. For the clouds characterized as stratiform, bullet rosettes and their aggregates were predominant at temperatures from about -40 to -25C, to plates and their aggregates as temperatures warmed from -20 to -8C, and frequently observed needles and their aggregates warmer than -5C. Below -40C, particles were often single pristine plates and

Ice particle mass and cross-sectional areas, together with their drag coeffcients, are needed for calculating the fallspeeds. Particle masses were obviously higher for the complex, often rimed ice crystals observed in the convective outflow ice clouds.

The masses are calculated in the following way. Direct measurements of the total condensate water content were measured in nine of the ten field programs. Because mixed-phase regions have been excluded, the condensate water content is the ice water content. The total mass—ice water content, is the integration of the particle mass across the particle size distribution (PSD). PSDs beginning at 2–10 μm for the <–60 C samples and larger than about 50 μm for the warmer clouds extending to several cm were measured. Corrections to reduce particle counts from shattering on the forward surfaces of the imaging probes were conducted using particle interarrival times.

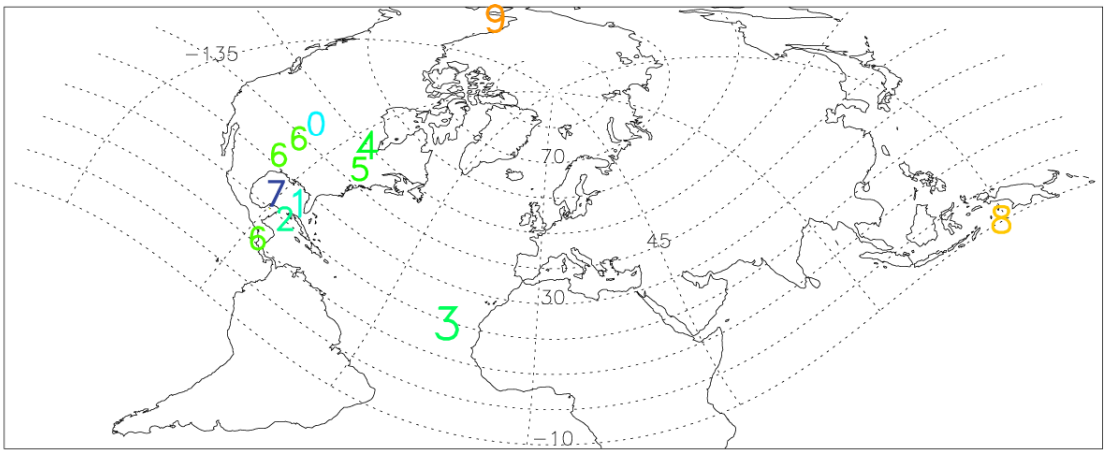

0–ARM: ARM 2000, Atmospheric Radiation Measurement (ARM) Field Campaign, 2000
1: CF: CRYSTAL–FACE, The Cirrus Regional Study of Tropical Anvils and Cirrus Layers – Florida Area Cirrus Experiment, 2002
2: TC4: The Tropical Composition, Cloud and Climate Coupling (TC4) Field Campaign, 2007
3: NAM: NAMMA – The NASA African Monsoon Multidisciplinary Analyses Campaign, 2006
4: AIRS: AIRS_2, Alliance Icing Research Study II, 2003–2004
5: C3VP: Canadian CloudSat/CALIPSO Validation Program, 2006–2007
6: Rep: Replicator Observations, First ISCCP Research Experiment (FIRE)–2, 1991
7: SV, Subvisual: Experiments with CF and pre–AURA Validation Experiment, 2002 and 2004
8: SCT, SCOUT: StratosphericDClimate Links w/Emphasis on the Upper Troposphere/Lower Stratosphere, 2003
9: MPACE: Mixed–Phase Arctic Cloud Experiment, 2004

Figure 1: Field projects and locations of the projects used in the observations.

Using various assumed ice particle power-law type mass-dimensional relationships of the form $m=aD^b$, and an analysis of the ice particle geometric properties —the fractal dimension, together with the PSDs, provided us an opportunity to derive the *a* and *b* coefficients. We were able to estimate a value of *b~2.1*. A value of a~0.006 (cgs units) gave reasonable estimates of the IWCs for the warmer temperature observations and the Schmitt and Heymsfield (2009) relationship based on a similar analysis for the colder ones (see Fig. 2). But, the way I've estimated a more accurate coefficient *a* for each PSD is to compare the IWC given by the value of *a* above and to scale it by the ratio of the measured IWC to the IWC derived by the value noted above. This should provide a good estimate of the true particle masses and account for formation in convective situations, etc.

Particle cross-sectional area is also needed for the calculations of ice particle fallspeeds. The area ratio, A_r, given by the ratio of the particle area divided by the area of a sphere that completely encloses the projected area of a particle,

$$A = A_r(\pi / 4)D^2$$

is found for every particle imaged by the 2D probes for temperatures warmer than -60C and from the small particle probes used in the low temperature observations.

For temperatures above –60 C, an average A_r value is found for each size bin of each 2D PSD and then a fit in the form

$$A_r = \alpha D^{\beta}$$

is used to specify the particle area ratios that coincide with a given PSD. For a sphere, α=1 and β=0 The Replicator images are used to derive α and β in (9). For the PA and SCOUT data, we use the Schmitt and Heymsfield (2009) relationship. They used combination of an exponential and power-law function covering the full size range limits but these are difficult to compare with (9). We use their relationships over the size range from the minimum to maximum measured for each PSD and then fit a power-law relationship for that PSD that covers the measured size range.

The values of α increase with temperatures from -60 to 0C (Fig. 3a). This increase as the temperature increases towards 0C indicates that the particles are increasingly filled in, possibly reflecting a trend from more pristine particles (e. g., columns, bullet rosettes) at low temperatures to aggregates and more complex 2 and 3D forms at warmer temperatures. Similarly, the value of β approaches 0 as temperature increases from -60 to 0C, thus indicating a value decreasing toward that of a sphere. (Fig. 3b). These trends are reflected in the nearly monotonic relationship between α and β (Fig. 3c), with increasing values of α associated with increasing β and thus more of a tendency for filled in particles at the larger β values.

Drag coefficients, the third necessary ingredient in the calculation of the terminal velocity, draw upon the recent non-dimensional parameterization that draws on the area ratio by Heymsfield and Westbrook (2010). An implicit assumption in earlier studies is that particles of all sizes contribute to the total precipitation rate, a premise that produces considerable error in snow precipitation rates, especially when a V_t-D power-law type relationship is extrapolated well beyond its measurement range. Consequently, I use a new and more objective technique to develop V_t-D relationships across the relevant sizes. I calculate the distribution of the IWC per size bin across each PSD from the m(D) relationship and the total IWC for all bins combined. The result is a distribution of the contribution of each bin size to the IWC for each PSD. Examination of the bin size-dependent contribution to the IWC reveals that it is not uniformly distributed across all sizes but rather is a distribution with a clearly defined peak somewhere near the mid-diameter of the PSD. For each PSD, I've found the bin diameter at the peak of the IWC(D)-D distribution and then find the diameter range either side of the peak that yields 70% of the total IWC. The quantitative amount of 70% is chosen arbitrarily, but it is well within the diameter range where the V_t-D relationship can be represented reliably with a power-law form (corresponding curve plotted in each panel). Not surprisingly, the range of sizes producing 70% of the total IWC is much smaller for the lower temperature cases than for the higher ones. For the small particles, the V_t approaches the values for Stokes ice spheres, as expected, but fall well below an extrapolation of the Locatelli and Hobbs (1974, hereafter LH74) curve used in many models. The fall velocities of the larger particles in the convectively generated clouds tend to be larger than for in situ-generated clouds for the same diameter because the masses are higher than in the stratiform situations.

I can compile a data set of the V_t*s* for those particle sizes that contribute 70% of the total IWC for each field program and derive them for a common pressure of 1000 hPa to compare further our observations to those of LH74 and to each other. Although I could have considered 70% of the IWC and total particle area in developing the relationships, this process works well for the warmer temperatures where both parameters fall in about the same range of sizes and for the lower temperatures the smaller particles behave as Stokes particles. The V_t for particles in the 500 to about 3000 μm size range for the stratiform cases corresponds quite closely to LH74 in their measurement

size range of 2 to 10 mm, but underestimates them by a factor of 2 or 3 for the convectively-generated ice.

Using the 70% IWC criteria to define the most important range of V_t's for climate studies, the V_t's for four pressure levels—1000, 800, 600, and 400 hPa, representing the range corresponding to sea level and most ice cloud heights—have been derived. The motivation is to develop V_t-D relationships that can be readily adjusted to include pressure levels for most subfreezing cloud temperatures. Figure 4 shows the results for pressure levels of 400 and 800 hPa, partitioned by convective and stratiform cloud types. Several power-law type curve fits are included over size ranges where these fits are well represented by power-law relationships: sizes smaller than 40 μm where $V_t \sim D^{2.0}$; intermediate sizes where $V_t \sim D^{0.9}$; and large sizes where $V_t \sim D^{0.2}$. The flatness of the curve for the largest size range is consistent with earlier measurements indicating that the fall speeds are relatively constant with size for >1 mm diameter aggregates (e. g., LH74 with b=0.16). The smallest size range corresponds to Stokes-size particles.

The results shown in Fig. 4 can be generalized by developing V_t-D power-law type relationships as in Fig. 4, for a pressure level of 1000 hPa, then by factoring in a multiplicative pressure dependent correction term. For a pressure level of 1000 hPa, for designated "stratiform" clouds:

$$V_t=0.0028D^{2.00},\ D<43\mu\text{m}$$

$$V_t=0.2079D^{0.8528},\ 43<D<823\mu\text{m}$$

$$V_t=22.03D^{0.1581},\ D>823\mu\text{m}$$

and for designated "convective" clouds:

$$V_t=0.0028D^{2.00},\ D<41\mu\text{m}$$

$$V_t=0.1098D^{1.0094},\ 41<D<771\mu\text{m}$$

$$V_t=10.18D^{0.3280},\ D>771\mu\text{m}.$$

Assuming pressure levels of 800, 600 and 400 hPa, we derived the pressure correction term relative to a pressure of 1000 hPa, and represented it in the following analytic form:

$$V_t(P)/V_t(1000)=C_0+C_1\ln(D).$$

Note that the pressure correction is size dependent and again is much below the non-size-dependent corrections used in earlier studies. Also, the terms C_0 and C_1 above are each pressure dependent.

Drawing upon the curve fits as in Fig. 4, I derived a single pressure-dependent correction C that is multiplied by the $V_t(D)$ to get the pressure effects,

$$C=C_0(P)+C_1(P)\ln(D),$$

where the following analytic terms are derived:

C_0=–1.23+0.325ln(P),

C_1=0.670–0.097ln(P).

I believe that these new relationships are much closer to reality than has been available before and I hope that ECMWF considers them in their future ice cloud modeling activities.

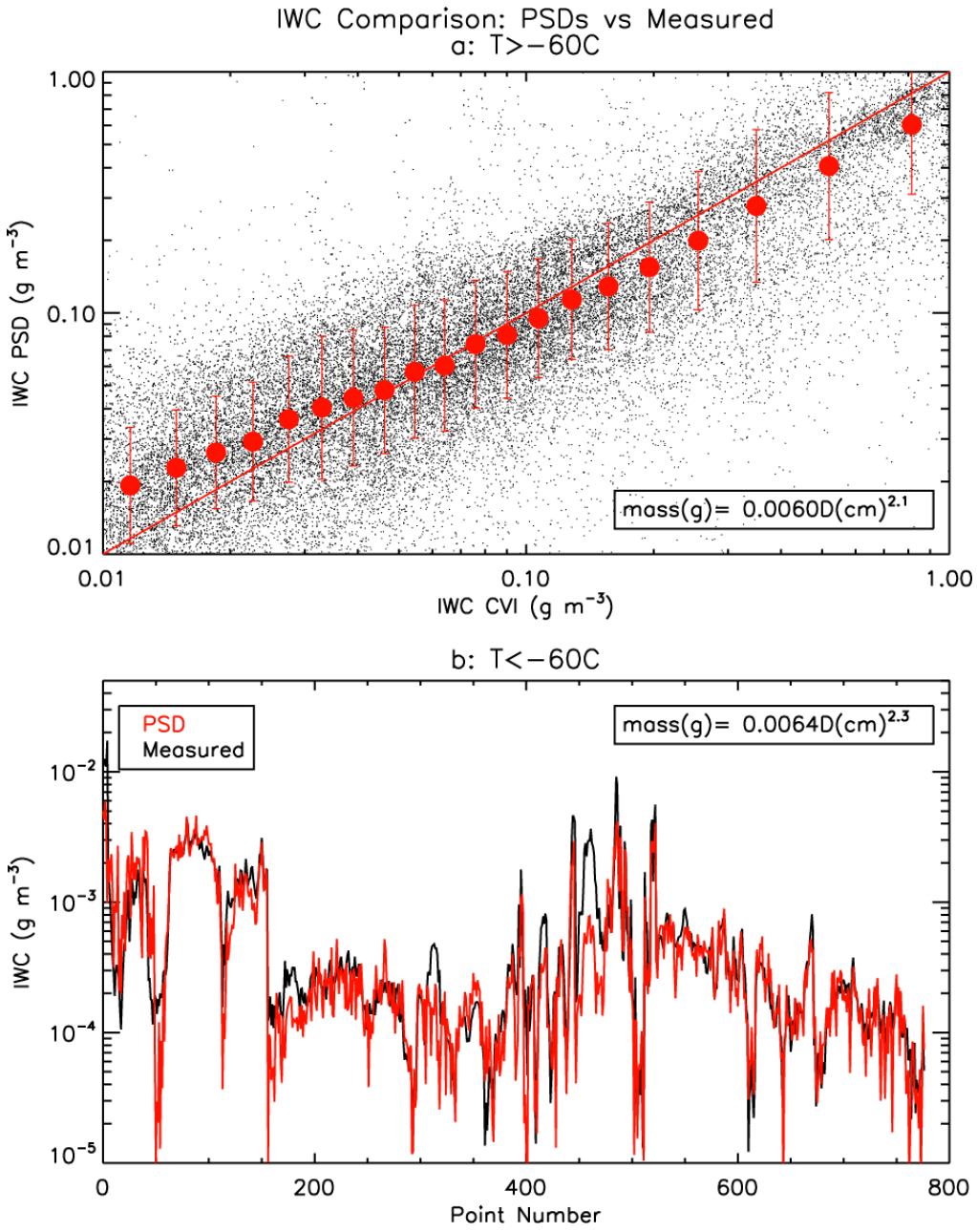

Figure 2 (a): Comparison of the IWC derived from the PSDs with one assumed mass-diameter relationship (shown) to those measured by the CVI, for the data at temperatures –60 C and above. (b) IWCs calculated from the PSDs and m(D) relationship from Schmitt and Heymsfield (2009), for data from temperatures below –60 C.

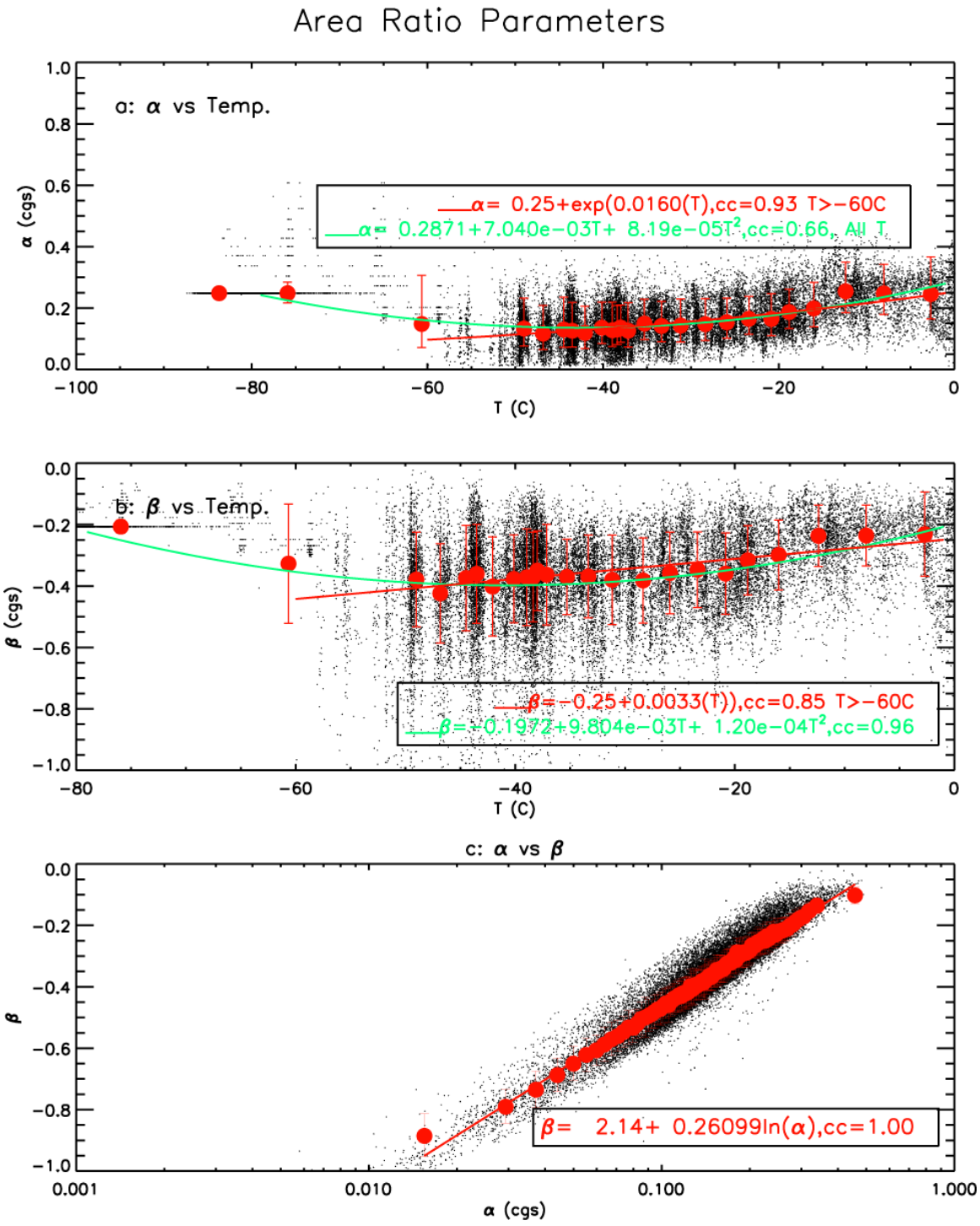

Figure 3: Coefficients in the area ratio-size relationship given by the form $A_r = \alpha D^{\beta}$ where D is in cm, as a function of temperature. (a, b) α and β. (c) The relationship between the two parameters. Curve fits to the data are shown.

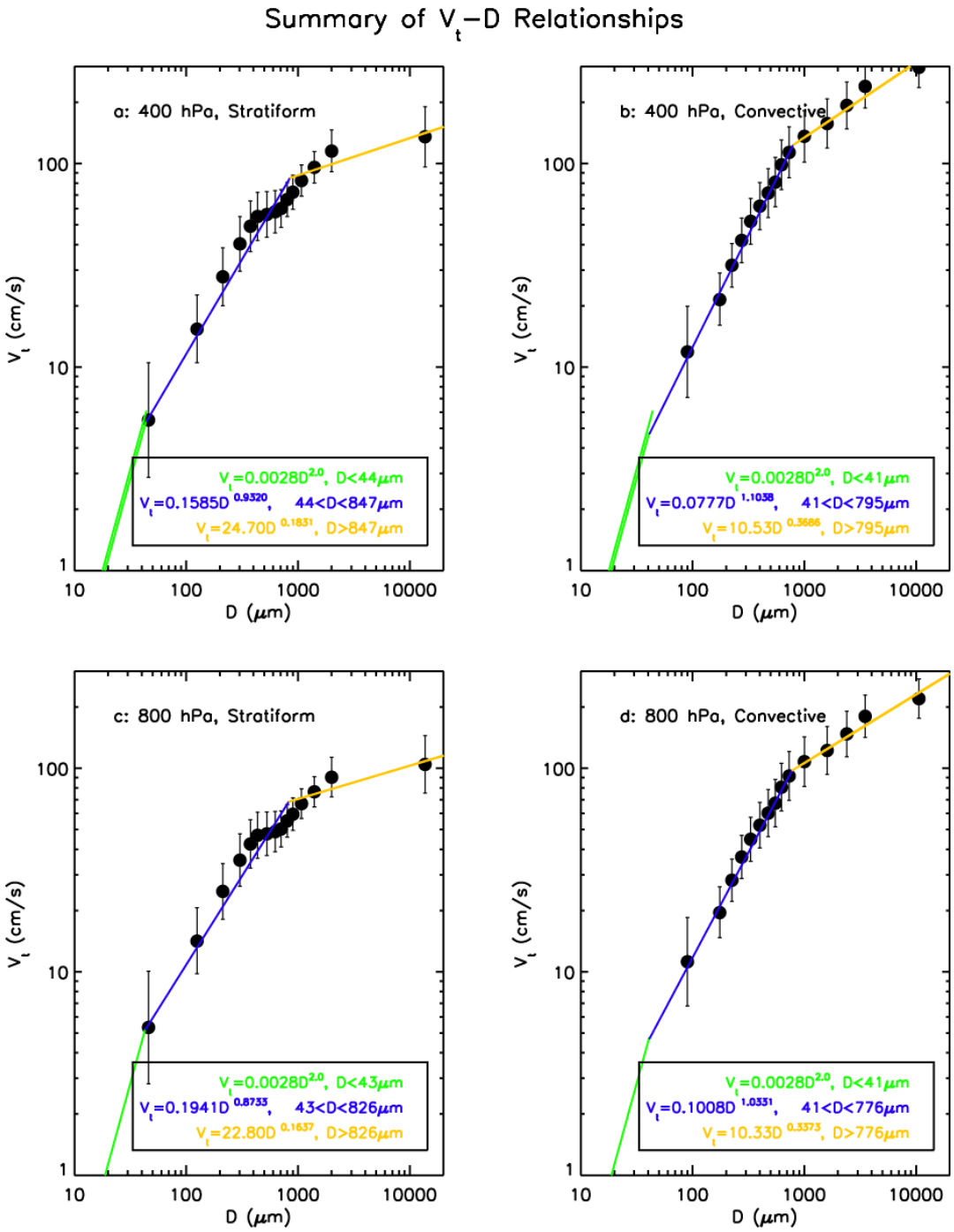

Figure 4: Average terminal velocities as a function of particle diameter for (left) stratiform and (right) convectively defined ice clouds, and pressure levels (a, b) 400 hPa and (c, d) 800 hPa. Power-law relationships are fitted to the calculations in three intervals of particle size.

References

Jakob, C., 1994: The impact of the new cloud scheme on ECMWF's integrated forecasting system (IFS). In *ECMWF/GEWEX Workshop on Validation and Assimilation of Clouds,* 31 October to 4 November 1994, pages 277-294, Shinfield Park, Reading.

Schmitt, C. G., and A. J. Heymsfield, 2009: The size distribution and mass weighted terminal velocity of low-latitude tropopause cirrus crystal populations. *J. Atmos. Sci.*, 66, 2013–2028.

Heymsfield, A. J., and C. D. Westbrook, 2010: Advancements in the estimation of ice particle fall speeds using laboratory and field measurements. *J. Atmos. Sci.*, 67, 2469–2482.